MOUNTAIN WAVE RELATED TURBULENCE DERIVED FROM SONIC ANEMOMETERS AND AN ELASTIC BACKSCATTER LIDAR

Željko Večenaj[1], Stephan F.J. De Wekker[2] and Vanda Grubišić[3]

[1]Department of Geophysics, Faculty of Science, Zagreb, Croatia
E-mail: *zvecenaj@gfz.hr*
[2]Department of Environmental Sciences, University of Virginia, USA
[3]Department of Meteorology and Geophysics, University of Vienna, Austria

Abstract: A case study of mountain wave related turbulence during the Terrain-induced Rotor EXperiment in the Owens Valley is presented. Large spatial and temporal variability in aerosol backscatter was observed in the valley atmosphere associated with mountain wave activity. The corresponding turbulence structure along and across the valley was investigated using data collected by three 30 m NCAR towers equipped with 6 levels of ultrasonic anemometers. Time series of turbulent kinetic energy (*TKE*) show much higher levels of *TKE* in the valley center than on the sloping western part of the valley. An analysis of the *TKE* budget shows that mechanical production of turbulence is dominant and balanced by turbulent dissipation in central parts of the valley. The data and analysis from this case study can be used to evaluate and improve turbulence parameterization schemes in atmospheric numerical models.

Keywords: T-REX experiment, turbulent kinetic energy, budget equation, dissipation rate

1 INTRODUCTION

Terrain-induced Rotor Experiment (T-REX) was conducted during spring 2006 in Owens Valley, California. During the Intensive Observation Period 1 (IOP 1) from 0000 UTC on 02 March to 1500 UTC on 03 March 2008 a transition occurred from a quiescent to a disturbed boundary layer accompanied by large spatial inhomogeneities in the aerosol backscatter (De Wekker and Mayor, 2009).The turbulence structure near the surface during these transitions is poorly known and potentially important for the modification of mountain wave activity and the generation of rotors and subrotors on the lee-side of mountains.

Turbulent kinetic energy (*TKE*) is produced and destructed by various processes that are explained by the different terms in the *TKE* budget equation (e.g. Stull, 1988). One of the terms is the eddy dissipation rate (ε) which is parameterized in numerical models (e.g. Mellor and Yamada, 1974) and used in turbulence nowcasting at the airports (e.g. Frech, 2007). By quantifying both the *TKE* and ε, parameterization schemes that are used in these models can be evaluated and potentially improved.

2 FIELD EXPERIMENT, INSTRUMENTATION AND DATA

Data from three towers from the Integrated Surface Flux Facility (ISFF) installed by NCAR and from the Raman-shifted Eye-safe Aerosol Lidar (REAL) are used in this study. Figure 1 shows the map of the site with the towers and REAL indicated.

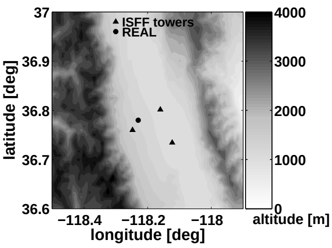

Figure 1. The map of the area of interest together with the locations of the towers and the lidar.

The western tower (WT) was located on the alluvial slope on the western side of Owens Valley. The central tower (CT) and the south tower (ST) were located along the valley's central axis extending from NNW to SSE. Each tower was 35 m tall and instrumented with CSAT3 ultrasonic anemometers collecting data with a sampling rate of 60 Hz at heights of 5, 10, 15, 20, 25 and 30 m. REAL was installed between WT and CT on the alluvial slope providing an undisrupted view in all directions within its range. Vertical and horizontal scans were made using REAL (De Wekker and Mayor, 2009).

3 RESULTS

In Cartesian system, the *TKE* is defined as a sum of variances of all three wind components:

$$TKE = \frac{1}{2}\left(\overline{u'^2} + \overline{v'^2} + \overline{w'^2}\right) \qquad (1)$$

The *TKE* budget equation is expressed as (e.g. Stull, 1988):

$$\frac{\partial TKE}{\partial t} = \underbrace{\frac{g}{\Theta_v}\left(\overline{w'\theta'_v}\right)}_{II} - \underbrace{\overline{u'w'}\frac{\partial U}{\partial z}}_{III} - \underbrace{\frac{\partial\left(\overline{w'TKE}\right)}{\partial z}}_{IV} - \underbrace{\frac{1}{\rho}\frac{\partial\left(\overline{w'p'}\right)}{\partial z}}_{V} - \underbrace{\varepsilon}_{VI} \qquad (2)$$

I

Term I represents a local storage of *TKE*. Term II is the buoyant production/consumption term depending on the sign of the heat flux ($\overline{w'\theta'_v}$). Term III denotes mechanical (shear) production term. Term IV describes the turbulent transport of *TKE* by the vertical velocity w of turbulent eddies. Term V is a pressure correlation term that shows how pressure perturbations redistribute *TKE* in the vertical. Finally, term VI represents the dissipation of *TKE* by molecular viscosity into heat.

Between 2345 UTC on 02 March and 0115 UTC on 03 March REAL detected interesting features that indicated presence of high levels of turbulence (De Wekker and Mayor, 2009). ISSF towers reveal that *TKE* indeed is strong along the valley (ST, Fig. 2c and CT; Fig. 2b) due to the influence of strong south-easterly flows along the valley. However, *TKE* is considerably weaker at WT (Fig. 2a). REAL data shows that downslope advection of stable stratified air occurs near the western tower leading to the low levels of turbulence there. The *in-situ* measurements do not capture the increased mixing above ~ 1 km revealed by REAL. REAL indicated that this increased mixing is caused by the interaction of the downslope flow and the SE flow along the valley. From Fig. 3 it is obvious that the mechanical term and ε are predominant and almost in balance at all mid-levels at the CT (Fig. 3b) and ST (Fig. 3c). In general, the values at WT are approximately 5 times smaller than at CT and ST, confirming that the turbulence is suppressed at WT. However, ε is noticeable larger than the sum of *TKE* production terms, i.e. mechanical shear and buoyancy, at WT. This indicates that the *TKE* was not produced locally but advected from elsewhere by the downslope flows.

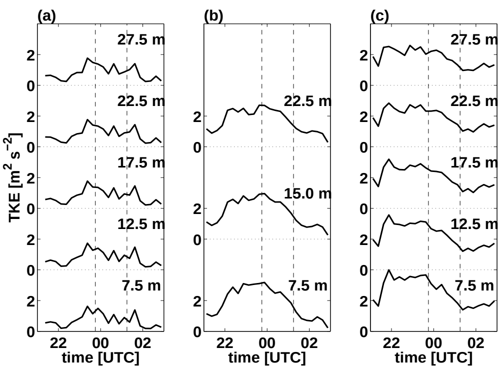

Figure 2. Temporal evolution of the *TKE* evaluated at various mid-levels at WT (a), CT (b) and ST (c). The heights of the various mid-levels are indicated in the figure. Vertical dashed lines depict the period of interest.

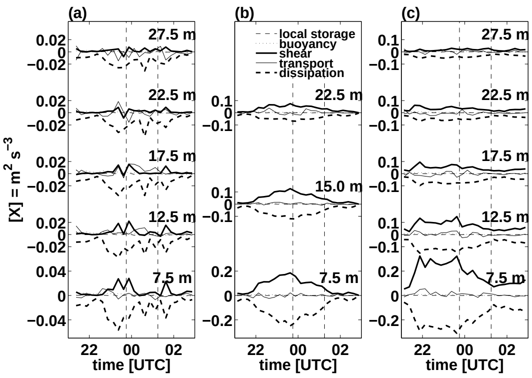

Figure 3. Temporal evolution of the terms from the *TKE* budget equation (equation 2 in text) evaluated at the mid-levels at WT (a), CT (b) and ST (c). The heights of the mid-levels are indicated in the figure.

4 SUMMARY

During T-REX IOP 1, a transition from a quiescent to a disturbed boundary layer is accompanied by large variability in space and time of aerosol backscatter and turbulent kinetic energy. Stably stratified downlope flows suppress the *TKE* on the western side of the valley while the *TKE* is enhanced in the central part of the valley, where a strong interaction between downlope flows, channelled along-valley flows and mountain waves occurs. At the along-valley locations locally produced shear-driven turbulence is balanced by turbulent dissipation while advection effects play an important role at the western slope location. This study exemplifies the benefit of combined in-situ and remote sensing measurements in providing an improved understanding of temporal and spatial turbulence variability in complex terrain.

Acknowledgements:

This study is partially supported by the Croatian Ministry of Science, Education & Sports, projects BORA No. 119-1193086-1311. This work was started while ZV was a visiting student at the University of Virginia.

REFERENCES

De Wekker S.F.J. and S.D. Mayor, 2009: Observations of atmospheric structure and dynamics in the Owens Valley of California with a ground-based, eye-safe, scanning aerosol lidar. J. Appl. Meteor. Climat.In press.

Frech, M., 2007: Estimating the turbulent energy dissipation rate in an airport environment. Boundary-Layer Meteorol. **123**, 385–393.

Mellor, G.L. and T. Yamada, 1974: A hierarchy of turbulence closure models for planetary boundary layers. J. Atmos. Sci. **31**, 1791-1806.

Stull, R.B., 1988: An Introduction to Boundary Layer Meteorology, Kluwer Academic, 666 pp.